Proactive Demand Participation of Smart Buildings in Smart Grid

Tianshu Wei, *Student Member, IEEE,* Qi Zhu, *Member, IEEE,* Nanpeng Yu, *Member, IEEE*

Abstract—Buildings account for nearly 40% of the total energy consumption in the United States. As a critical step toward smart cities, it is essential to *intelligently manage and coordinate* the building operations to improve the efficiency and reliability of overall energy system. With the advent of smart meters and two-way communication systems, various energy consumptions from smart buildings can now be coordinated across the smart grid together with other energy loads and power plants. In this paper, we propose a comprehensive framework to integrate the operations of smart buildings into the energy scheduling of bulk power system through *proactive building demand participation*. This new scheme enables buildings to proactively express and communicate their energy consumption preferences to smart grid operators rather than passively receive and react to market signals and instructions such as time varying electricity prices. The proposed scheme is implemented in a simulation environment. The experiment results show that the proactive demand response scheme can achieve up to 10% system generation cost reduction and 20% building operation cost reduction compared with passive demand response scheme. The results also demonstrate that the system cost savings increase significantly with more flexible load installed and higher percentage of proactive customers participation level in the power network.

Index Terms—Smart building, smart grid, demand response, proactive participation, MPC control, energy cost reduction

1 Introduction

Buildings account for nearly 40% of the U.S. primary energy consumption and 70% of the electricity use [1]. To build smart cities with efficient and reliable energy systems, it is critical to intelligently manage various energy demands of buildings *and* coordinate such management across buildings in the smart grid.

A key aspect in improving building energy efficiency is to leverage the scheduling flexibility provided by various energy demand loads in buildings, including HVAC (heating, ventilation and air conditioning), plug loads, and emerging loads such as EV (electric vehicle) charging, etc. In particular, HVAC system consumes around 50% of the total building energy consumption [1]. Its energy demand may change based on the dynamic physical environment (e.g., outside air temperature and sun radiation) and building occupancy activities. It also needs to be carefully managed to satisfy the building temperature and air flow requirements. The building thermal flywheel effect allows temporarily unloading the HVAC systems without immediate impact on building occupants [2], and therefore provides significant flexibility in managing the demand. Furthermore, battery storage has been increasingly used at building level to store energy during off-peak hours (or from renewable energy sources) and release energy at peak hours. This provides additional flexibility for building energy scheduling.

To leverage the flexibility provided by building energy loads such as HVAC systems, various energy management methods have been proposed, however they mostly focus on developing load control algorithms to reduce energy consumption and shave peak demand for individual buildings. There are also a variety of demand response (DR) strategies in the literature for leveraging such flexibility to improve electricity market efficiency. However, they are mostly price-based or incentive-based, in which the building energy management system passively follows the electricity price and load reduction signals from the utilities [3].

Indeed, little work has been done to consider integrating the intelligent building energy scheduling process with the electricity market economic dispatch strategy in a holistic framework. Currently, almost all demand response customers still schedule their own energy demand by passively reacting to the real-time varying price and demand reduction instructions dispatched from market system operator [4]. This passive and single-direction communicating demand response mode greatly limits the potential effectiveness of demand response strategy in leveraging the tremendous amount of building energy load flexibility. Such structural rigidity results in low customer engagement [3], and is part of the reason why the U.S. demand response penetration level is only at 6% [5].

As estimated in the FERC demand response report [6], the total peak power demand in the U.S. can be reduced by 150 GW assuming the participation of the entire customers. To further exploit the huge potential of demand response in improving power system efficiency and facilitate customers' engagement level in electricity market, in this paper, we propose an innovative demand response scheme based on *proactive demand participation from smart buildings*. Under this proactive demand response scheme, physical dynamic models, embedded in intelligent building energy scheduling agents, are able to capture the characteristics of various loads and predict buildings' operating states evolution. In electricity market, the intelligent energy scheduling agent in each individual building submits demand bids for its electricity consumption based on the electricity price forecast and current operating states. Then the demand bid information is aggregated by distribution system operators at the substation level and sent to the wholesale market operator. After receiving all demand bids and supply offers, the wholesale market operator solves the security constrained

economic dispatch (SCED) problem to clear the demand and supply in electricity market. Finally the market clearing results (i.e., electricity prices and dispatch operating points) are disaggregated into individual customer's dispatching quantity. Those electricity dispatching instructions are sent back to each individual customer. The customers strictly follow their dispatching quantities to operate various types of load inside buildings.

The *main contribution of this paper* is to propose and develop above-mentioned demand response scheme with intelligent scheduling and proactive participation of smart buildings. This includes the following aspects:

- At the building scheduling level, we construct a building thermal dynamics model to characterize heat transfer process and forecast building temperature evolution. We develop a model predictive control (MPC) based algorithm to intelligently schedule the HVAC system and battery usage for reducing energy cost. Then, based on the building scheduling algorithm, we generate a *demand bid curve* for each building to quantify its energy load flexibility under various price forecasts.
- At the power system level, we develop algorithms to first aggregate individual demand bid curves from buildings at the substation (distribution network) level and then solve the SCED problem at the wholesale market (transmission network) level to maximize the sum of total surplus of all customers and power generation companies. The SCED optimization determines the electricity price and quantity, which are then disaggregated to the individual building customer level.
- We conduct a set of experiments on an IEEE 30-bus network to evaluate the effectiveness of our proposed proactive demand response scheme.

Compared with existing passive demand response strategies, our proactive scheme enables building customers to actively participate in the electricity market operation, instead of just passively following demand reduction signals and reacting to real-time prices. The experiment results demonstrate that our approach can greatly reduce power system generation cost and building operation cost.

The remainder of this paper is organized as follows. Section 2 summarizes some of the existing approaches on building energy management and DR programs in the literature. Section 3 introduces the structural overview of our proposed framework with proactive demand participation from smart buildings. Section 4 presents design details of the framework. Section 5 introduces a baseline passive demand response mechanism as a comparison reference. Section 6 shows experiment results and conducts critical analysis of our proposed approach, and Section 7 concludes the paper.

2 Related Work

Many current research efforts focus on the design of price-based demand response models and control strategies [7]. Various price-based DR pricing strategies have been proposed [8], such as real-time pricing (RTP) [9]–[12], critical peak pricing [13], [14], peak load pricing [15], [16], peak day rebates pricing [17] and time-of-use [18]–[20]. Among the existing price-based demand response frameworks, the iterative real-time pricing mechanism [10] is shown to be one of the most effective and efficient approaches in managing distributed demand response resources. In the iterative RTP approach, system operators (or utility companies) and customers iteratively compute electricity prices and optimal electricity consumptions until a suitable set of prices and energy consumption schedules is reached. Due to the inflexibility of the communication scheme, it usually takes a high number of iterations [21] to achieve the optimal allocation point, assuming constant external conditions during the entire process. When applied in practical electricity market environment, the iterative RTP mechanism suffers from two critical drawbacks. First, the combination of a high number of iterations and the complexity of unit commitment problem in a regional electricity market makes the iterative negotiation process too slow for real-time operations. In some cases, the convergence of the algorithm cannot be guaranteed with a lossy and delayed communication platform. Second, we have to assume that both generation company agents and consumers adhere to the same consumption and bidding strategy without the ability to learn and adjust based on external shocks and past bidding experiences.

Although there have been numerous studies on locational marginal pricing in wholesale power market, there has not been much literature that focuses on retail market pricing and designing interface between retail market and wholesale market. In [22], the authors propose a distributed approach to derive retail market spot pricing in a radial distribution network. To enhance efficiency of distributed generation, nodal pricing mechanism for distribution networks is developed in [23]. A novel pricing mechanism for locational marginal pricing with significant distributed generation penetration is constructed in [24]. An iterative approach is presented in [25] to integrate the transmission and distribution grid together with residual demand modeling in transmission network [26]. None of these existing pricing mechanisms allows joint optimization of flexible energy demands and generation power plants in an integrated framework with price sensitive demand bids derived from building control models.

At the individual customer level, there has been a variety of work on scheduling flexible energy loads such as HVAC system and EV charging for demand response. For energy-efficient HVAC control, a set of system models and algorithms is proposed in [27]–[33]. In [27], a non-linear model of the overall cooling system is proposed, and an MPC scheme for minimizing energy consumption is developed. In [28], a system model is proposed that is bilinear in inputs, states and weather parameters, and a form of sequential linear programming (SLP) is developed for solving the control optimization problem. In [30], a building thermal behavior is modeled as RC networks and validated against historical data, and a tracking linear-quadratic regulator (LQR) is proposed for HVAC control. The work in [32] uses the similar building model as in [30], and proposes a set of HVAC control algorithms that address the sensing data inaccuracy using unscented or extended Kalman filters. In addition to scheduling energy loads, there are also approaches proposed for scheduling heterogeneous energy sources such as battery storage at individual customer level [34]–[38].

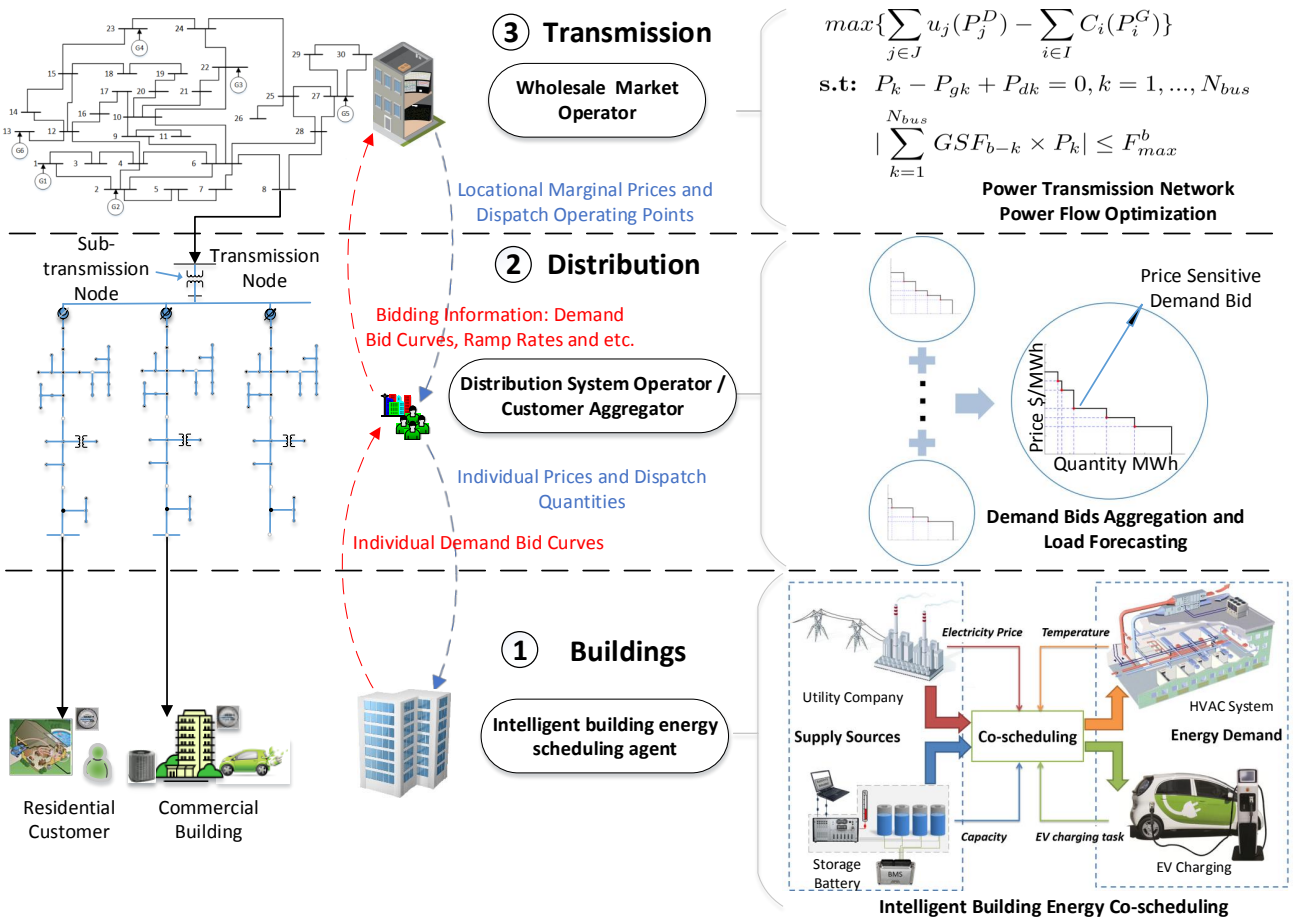

Fig. 1: Integrated Market Operations Framework with Proactive Demand Participation

Despite these approaches for scheduling HVAC control, battery storage and other energy sources, little work exists for combining the demand response consideration at individual customer level together with the optimization at network level, which is the focus of our approach.

3 Overview of Proposed Framework

Our proposed integrated market operations framework with proactive demand participation from smart buildings is illustrated in Fig. 1. The framework integrates demand response and network optimization across three levels of the smart grid – individual (building) customers, distribution system, and transmission system – through the interactions of three key decision making entities, including intelligent building energy scheduling agent, distribution system operator/customer aggregator and wholesale market operator.

Intelligent Building Energy Scheduling Agent: At the building customer level, intelligent energy scheduling agent is designed to reduce energy cost and enable proactive demand participation. First, as part of the building automation and control system, the agent minimizes the building operating energy cost by scheduling the energy consumptions of various subsystems and controlling the usage of heterogeneous energy supply sources, while satisfying the requirements from building occupants. In this work, we address the scheduling of HVAC systems and battery storage systems with an MPC control algorithm.

Then, the agent constructs demand bid curves that capture the potential building energy demand under various possible grid electricity price. Those demand bid curves will then be sent to the distribution system operator/customer aggregator via wide-area network. After the day-ahead and real-time markets are cleared by the electricity wholesale market operator, the building intelligent agent will receive the dispatch operating points in the same way as a regular power plant. By following the total electricity dispatch instruction, the intelligent agent will then coordinate various flexible loads to determine the amount of electricity that should be allocated to each of them.

Distribution System Operator/Customer Aggregator: The number of building customers in a regional electricity market could easily add up to millions. It is inefficient and impractical to deal with every individual customer's demand bid curve directly in the electricity market. To reduce the complexity of unit commitment and economic dispatch process when flexible load demand bids are considered, distribution system operator/customer aggregator needs to

accurately aggregate individual demand bid curves at the substation level. Namely, the distribution system operator needs to find a set of equivalent overall demand bids which reflect integral demand bid characteristics of all individual customers at the transmission interconnection node while considering the physical models of distribution system. In the distribution system, there could exist participations from both proactive customers and passive customers who do not participate in the proactive demand bid program. To deal with the mixed customer structure, it is essential for distribution system operator/customer aggregator to predict the flexible load demand from passive customers based on smart meter data and current weather information.

The demand bid aggregation process follows an iterative process if the distribution network is radial. The load at downstream node could be related to upstream node by considering distribution network losses [22]. The locational marginal price (LMP) at the downstream nodes could depend on the transmission interconnection nodes when marginal distribution losses due to power injection at the downstream node is considered [23]. Finally, the aggregated demand bid information will be incorporated into the day-ahead and real-time market clearing process. After these markets are cleared, the distribution system operator is responsible for disaggregating the distribution system dispatch operating point into individual customers.

Wholesale Market Operator: Currently, in most independent system operators' five-minute real-time operations, demand is treated as fixed injection into the power network. The wholesale market operator typically uses very short-term load forecasting algorithm to estimate total load in a region and then disaggregates the total load to individual nodes based on load distribution factors estimated from state estimation solutions. In our integrated market operations framework, the distribution system operators will submit demand bids at each transmission interconnection point as described above. The aggregated demand bid represents overall willingness to pay of all customers under the same pricing node. Therefore, apart from minimizing the total purchase cost of energy and ancillary services, the market operator will also try to maximize the sum of expected surplus of both generators and customers. The wholesale market operator is responsible for sending the dispatch operating points of the aggregated demand bids back to the distribution system operator.

4 Design of Proposed Framework

In this section, we introduce the design details of our proposed framework. In subsection 4.1, we present the intelligent energy scheduling algorithm at the building customer level, the creation and aggregation of demand bid curves for individual buildings. In subsection 4.2, we present the market operation optimization at the network level and disaggregation of dispatching points. Subsection 4.3 summarizes our proposed proactive demand participation scheme.

4.1 Intelligent Building Energy Scheduling and Demand Bid Curve Creation and Aggregation

At individual building customer level, it has been shown in our previous work that appropriately managing flexible energy loads such as HVAC systems and battery storage can effectively reduce both peak power demand and total energy cost of buildings [39], [40]. Furthermore, it is essential to control the HVAC energy consumption (by turning on/off air conditioning and changing air flow volume) and the usage of battery storage (by charging/discharging storage battery) *collaboratively in a holistic formation* to maximize building energy efficiency, as the two aspects have significant impact on each other [39].

Next, we will introduce our building thermal dynamics model, the MPC-based building energy scheduling algorithm that addresses both HVAC control and battery storage usage (refined from the proof-of-concept formulation in [39]), and the demand bid curve creation method.

4.1.1 Building Thermal Dynamics Model

We use a building thermal dynamics model similarly as in [30], [41], where a building is considered as a network. The building can be modeled by using two types of nodes: walls and rooms. Suppose there are in total n nodes, m of which are room nodes and $n-m$ are wall nodes. The temperature of the i-th wall is governed by equation (1).

$$C_{\omega_i}\frac{dT_{\omega_i}}{dt} = \sum_{j\in\mathcal{N}_{\omega_i}}\frac{T_j - T_{\omega_i}}{R'_{ij}} + r_i\alpha_i A_i q''_{rad_i}, i \in n-m \quad (1)$$

where T_{ω_i}, C_{ω_i}, α_i and A_i represent the temperature, heat capacity, absorption coefficient and area of i-th wall, respectively. R'_{ij} denotes the total resistance between wall i and adjacent node j. q''_{rad_i} is the radiative heat flux density on wall i. $\mathcal{N}_{\omega_i}$ denotes the set of all of neighboring nodes to node wall i. r_i is an indicator denoting whether wall i is a peripheral wall ($r_i = 1$) or not ($r_i = 0$). The temperature of the i-th room is characterized by the following differential equation (2).

$$\begin{aligned} C_{r_i}\frac{dT_{r_i}}{dt} = \sum_{j\in\mathcal{N}_{r_i}}\frac{T_j - T_{r_i}}{R'_{ij}} + \dot{m}_{r_i}c_a(T_{s_i} - T_{r_i}) \\ +\omega_i\tau_{\omega_i}A_{\omega_i}q''_{rad_i} + \dot{q}_{int_i}, i \in m \end{aligned} \quad (2)$$

where T_{r_i} , C_{r_i} and $\dot{m}_{r_i}$ denote the temperature, heat capacity and air mass flow into the room i, respectively. c_a is the specific heat capacity of air. A_{ω_i} is the total area of window on walls surrounding room i, τ_{ω_i} is the transmissivity of glass of window in room i. q''_{rad_i} is the radiative heat flux density radiated to room i, and $\dot{q}_{int_i}$ denotes the internal heat generation inside room i. $\mathcal{N}_{r_i}$ is the set of all of the neighboring nodes to room i. $\omega_i = 0$ indicates room i doesn't has any window, while $\omega_i = 1$ otherwise.

The above heat transfer differential equations of walls and rooms can be transformed into the following state space equation of the system dynamics (3).

$$\begin{aligned} \dot{\boldsymbol{x}}_{\boldsymbol{t}} &= f(\boldsymbol{x}_{\boldsymbol{t}}, \boldsymbol{u}_{\boldsymbol{t}}, \hat{\boldsymbol{d}}_{\boldsymbol{t}}) \\ \boldsymbol{y}_{\boldsymbol{t}} &= \boldsymbol{C}\boldsymbol{x}_{\boldsymbol{t}} \end{aligned} \quad (3)$$

where $\boldsymbol{x}_{\boldsymbol{t}} \in \mathbb{R}^n$ is the state vector representing the temperature of the nodes in the thermal network. $\boldsymbol{u}_{\boldsymbol{t}}$ is the input vector representing the air mass flow rate of conditioned air into each thermal zone. $\boldsymbol{y}_{\boldsymbol{t}} \in \mathbb{R}^m$ is the temperature of each thermal zones. $\boldsymbol{C}$ is a matrix of proper dimension used to

calculate thermal zones' temperature out of system states and $\hat{\boldsymbol{d}}_{\boldsymbol{t}}$ represents environment disturbance.

The original nonlinear model is used for state estimation, filtering and as a plant model to calculate the actual temperature evolution. While for control purpose, linear thermal dynamics model is used to reduce the complexity of the system. The original system dynamics model is linearized around the system operating point by using Jacobian linearization (details in [42]). The system equilibrium point is obtained by starting from an initial point and using a Sequential Quadratic Programming(SQP) search algorithm [43] until it finds the nearest equilibrium point to the specified system operating point (through solving a series of Quadratic Programming(QP) subproblems). We use zero-order hold to discretize the state space realization and derive the following discrete time LTI system (4).

$$\begin{aligned} \boldsymbol{x_{k+1}} &= \boldsymbol{A}\boldsymbol{x_k} + \boldsymbol{B}\boldsymbol{u_k} + \boldsymbol{E}\hat{\boldsymbol{d}}_{\boldsymbol{k}} \\ \boldsymbol{y_k} &= \boldsymbol{C}\boldsymbol{x_k} \end{aligned} \tag{4}$$

In equation (4), $\boldsymbol{A}$ is the system state coefficient matrix, $\boldsymbol{B}$ and $\boldsymbol{C}$ are control and output matrices respectively, while matrix $\boldsymbol{E}$ combines the impacts of various environmental factors on room temperature. In this work, we use the linear thermal dynamics model to capture the building heat transfer characteristics and develop the MPC-based building energy scheduling algorithm.

4.1.2 MPC-based Building Energy Scheduling Algorithm

Based on the building thermal dynamics model, we formulate an MPC-based control algorithm to co-schedule the HVAC control and the battery storage usage for reducing energy cost, while meeting HVAC system requirements on room temperature and airflow:

$$min \sum_{t=i}^{i+w-1} \left[\boldsymbol{p_g}(t) \cdot \boldsymbol{e_g}(t) + p_b \cdot \boldsymbol{e_b}(t)\right] \tag{5}$$

$$\forall t \in [i, i+w+1]$$

$$\textbf{s.t: } \boldsymbol{T_c}(t+1) = \boldsymbol{A} \cdot \boldsymbol{T_c}(t) + \boldsymbol{B} \cdot \boldsymbol{u}(t) + \boldsymbol{E} \cdot \hat{\boldsymbol{d}}(t) \tag{6}$$

$$U^- \leq \boldsymbol{u}(t) \leq U^+ \tag{7}$$

$$\boldsymbol{T}^-(t+1) \leq \boldsymbol{C} \cdot \boldsymbol{T_c}(t+1) \leq \boldsymbol{T}^+(t+1) \tag{8}$$

$$\boldsymbol{e_g}(t) = \boldsymbol{e_H}(t) + \boldsymbol{e_B}(t), \boldsymbol{e_g}(t) \geq 0 \tag{9}$$

$$\boldsymbol{e_H}(t) = c_1\boldsymbol{u}(t)^3 + c_2\boldsymbol{u}(t)^2 + c_3\boldsymbol{u}(t) + c_4 \tag{10}$$

$$-d_r \cdot \tau \leq \boldsymbol{e_B}(t) \leq c_r \cdot \tau \tag{11}$$

$$\boldsymbol{Soc}(t+1) = (1-\gamma) \cdot \boldsymbol{Soc}(t) + \rho \cdot \boldsymbol{e_B}(t) \tag{12}$$

$$E^- \leq \boldsymbol{Soc}(t+1) \leq E^+ \tag{13}$$

$$\boldsymbol{Soc}(t+1) = E_0, \text{if } t \bmod N = 0 \tag{14}$$

$$\boldsymbol{e_b}(t) = \begin{cases} |\boldsymbol{e_B}(t)| & \boldsymbol{e_B}(t) < 0 \\ 0 & \boldsymbol{e_B}(t) \geq 0 \end{cases} \tag{15}$$

The MPC-based algorithm is applied periodically. At each time instance t, it determines the optimal air flow volume trajectory $[\boldsymbol{u}(t), \boldsymbol{u}(t+1), \cdots, \boldsymbol{u}(t+w-1)]$ and battery charging/discharging trajectory $[\boldsymbol{e_B}(t), \boldsymbol{e_B}(t+1), \cdots, \boldsymbol{e_B}(t+w-1)]$ for a predicting window w (in our experiments the window is set to 24 hours). The optimization takes into account the electricity price forecasts and the building operation constraints such as room temperature constraints and battery storage charging/discharging restrictions. The room temperature within the predicting window is predicted based on the thermal dynamics model, the air flow volume trajectory, and the forecasted environmental disturbances. Once the optimal air flow volume and battery charging/discharging trajectories are determined, the MPC algorithm will implement the first entry $\boldsymbol{u}(t)$ and $\boldsymbol{e_B}(t)$ to control the HVAC system and operate the battery storage. Next, the time instance will advance to $t+1$ and the predicting window will advance by one time interval accordingly (in our experiments the time interval is one hour), and the MPC algorithm will be applied again.

Variables and parameters of the MPC formulation are listed in Table 1. Objective function (5) minimizes the total energy cost within the predicting window. The first term of (5) captures the energy consumption cost of the grid electricity, while the second term calculates the battery depreciation cost (based on battery manufacturing cost and battery maximum charging/discharging cycles). Battery discharging energy is denoted by $\boldsymbol{e_b}(t)$ and calculated in equation (15), where $\boldsymbol{e_B}(t) < 0$ represents battery discharging energy while $\boldsymbol{e_B}(t) > 0$ denotes battery charging energy. As shown in objective function (5), the battery depreciation cost is calculated during the battery discharging process. Equation (6) follows equation (4) and calculates the temperature of building thermal zones, where $\hat{\boldsymbol{d}}(t)$ is the environment disturbance vector that represents sun radiation intensity, ambient temperature, etc. Constraint (7) sets bounds for air flow input volume. Constraint (8) sets bounds for room temperature, which has to be satisfied for building occupants comfort. Constraint (9) sets the relation among grid electricity consumption $\boldsymbol{e_g}(t)$, HVAC energy consumption $\boldsymbol{e_H}(t)$, and battery charging/discharging energy $\boldsymbol{e_B}(t)$. The HVAC energy consumption $\boldsymbol{e_H}(t)$ is calculated in equation (10) as a function of air flow volume, and is based on the result from [44]. Constraint (11) restricts battery maximum charging/discharging rate. Equation (12) updates battery state-of-charge in the next interval by considering battery energy decay and round-trip efficiency. Constraint (13) sets the battery charging/discharging safety boundary. Constraint (14) is the battery end-of-day energy limit, which requires the battery to have the same initial state-of-charge condition when the next day begins.

4.1.3 Demand Bid Curve Creation

The intelligent building energy scheduling algorithm provides the optimal energy schedule of buildings for each time interval within the predicting window, given the forecasting information of real-time prices and environment disturbances. The pair of electricity demand and price forecast reflects the amount of electricity that customers would be willing to buy at the corresponding price in current time interval. As we increase (or decrease) the electricity price forecast for current time interval while keeping price forecasts for the rest of the time intervals fixed [1], the corresponding optimal energy consumption for current time interval decreases (or increases). These pairs of electricity price and quantity forecast explicitly quantify the flexibility

1. The real-time electricity price time series may exhibit autocorrelation, higher volatility and frequency of spikes, in which case a Markov regime switching model could be adopted to model the price series [45]. For simplicity, these stochastic factors are not modeled in this paper.

TABLE 1: MPC Algorithm Variables Definition

i	current time interval	w	predicting window length
τ	length of interval	N	total number of intervals
c_r	max charging rate	p_b	battery depreciation cost
d_r	max discharge rate	$\hat{\boldsymbol{d}}$	environment disturbances
$\boldsymbol{u}$	air flow volume	$\boldsymbol{p_g}$	electricity price vector
$\boldsymbol{T_c}$	node temperature	$\boldsymbol{e_H}$	HVAC energy demand
$\boldsymbol{e_g}$	building energy consumption		
$\boldsymbol{e_b}$	battery discharging energy		
$\boldsymbol{e_B}$	battery charging/discharging energy		
$\boldsymbol{Soc}$	battery state-of-charge		
E_0	battery initial state-of-charge		
γ	battery energy decay rate		
ρ	battery round-trip efficiency		
$\boldsymbol{A}, \boldsymbol{B}, \boldsymbol{C}, \boldsymbol{E}$	building thermal dynamics state space matrices		
U^-, U^+	air flow volume lower/upper bounds		
$\boldsymbol{T^-}, \boldsymbol{T^+}$	comfort zone temperature lower/upper bounds		
E^-, E^+	battery charging/discharging range bounds		
c_1, c_2, c_3, c_4	HVAC energy demand function coefficients		

of buildings in current time interval. The locus of points traced out by following the price-quantity pairs when we gradually increase price forecast for current time interval, forms the building's flexible load demand bid curve [3]. An example of an individual customer flexible loads demand bid curve in a specific time interval is shown as Fig. 2.

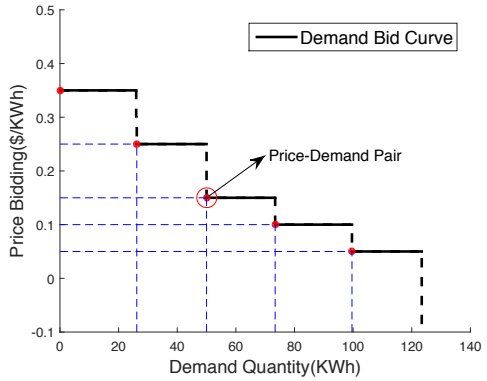

Fig. 2: Demand Bid Curve

We develop **Algorithm 1** to derive the demand bid curve of an individual customer. All notations used in Algorithm 1 are declared in Table 2. In the following, bold notations represent vectors and plain notations represent scalars.

As shown in Algorithm 1, calculating demand bid curve at current time interval i requires a price forecast vector $\boldsymbol{p_r}$ (whose length is the same as the predicting window size in MPC). P_{lower} and P_{upper} bound the possible price for current time interval i. Line 2 determines the number of distinct bid points. During each iteration, a possible price for interval i is stored into λ_i in line 4 and $\boldsymbol{p_r}$ is updated in line 5. Then line 6 runs MPC algorithm to compute the optimal energy scheduling $\boldsymbol{d}$ within current predicting window based on the updated price forecast profile $\boldsymbol{p_r}$. Line 7 and 8 store the possible price value and the corresponding demand bid into $\boldsymbol{w}$ and $\boldsymbol{P_j^d}$, respectively. Finally those

Algorithm 1 $\boldsymbol{P_j^d}$ = Demand_Curve$(i, \boldsymbol{p_r})$

1: Set P_{lower} and P_{upper}
2: $L \leftarrow (P_{upper} - P_{lower})/P_{incr} + 1$
3: **for** $l := 1$ to L **do**
4: $\quad \lambda_i \leftarrow P_{lower} + P_{incr} * (l-1)$
5: $\quad \boldsymbol{p_r}[i] \leftarrow \lambda_i$
6: $\quad \boldsymbol{d} \leftarrow$ MPC$(i, \boldsymbol{p_r})$
7: $\quad \boldsymbol{w}[l] \leftarrow \lambda_i$
8: $\quad \boldsymbol{P_j^d}[l] \leftarrow \boldsymbol{d}[1]$
9: **return** $\boldsymbol{P_j^d}$

TABLE 2: Algorithm 1 and 2 Variables Definition

λ_i	possible price at interval i	$\boldsymbol{p_r}$	electricity price vector
l	indices of bid points in demand bid curve		
L	total number of price points in demand bid curve		
P_{incr}	price increment		
$\boldsymbol{d}$	optimal energy scheduling within predicting window		
$\boldsymbol{w}$	customer willingness to pay for energy consumption $\boldsymbol{P_j^d}$		
P_{lower}	lower bound of price at interval i		
P_{upper}	upper bound of price at interval i		
n_j	number of buildings on bus j		
$\boldsymbol{P_j^d}$	energy consumption of individual demand bids set j		
$\boldsymbol{P_{j,k}^d}$	energy consumption of building k in demand bids set $\boldsymbol{P_j^d}$		
$\boldsymbol{P_j^D}$	energy consumption of aggregated demand bids set j		

isolated price-demand pairs are connected sequentially to form the demand bid curve of current time interval i.

4.1.4 *Individual Demand Bid Curve Aggregation*

The individual demand bid curves derived by Algorithm 1 need to be properly aggregated at substation level in order to solve the electricity market economic dispatch optimization problem. Without considering power losses in distribution lines, individual demand bid curves could be linearly added up to form the substation-level demand bid curve. This is shown in **Algorithm 2** with notations defined in Table 2. Line 1 in Algorithm 2 initializes the aggregated demand bids set $\boldsymbol{P_j^D}$. In line 3, all individual demand bids set $\boldsymbol{P_{j,k}^d}$ in demand bids set j are linearly added up to derive the aggregated demand bid set on bus j.

Algorithm 2 $\boldsymbol{P_j^D}$ = Bid_Aggregate$(j, \boldsymbol{P_j^d})$

1: $\boldsymbol{P_j^D} \leftarrow [\boldsymbol{0}]_{1 \times L}$
2: **for** $k := 1$ to n_j **do**
3: $\quad \boldsymbol{P_j^D} \leftarrow \boldsymbol{P_j^D} + \boldsymbol{P_{j,k}^d}$
4: **return** $\boldsymbol{P_j^D}$

4.2 Integrated Market Operations

4.2.1 *Network Optimization Formulation*

The real-time market clears the supply offers with demand bids by maximizing the sum of the surplus of generation companies and retail customers. In each time interval, the wholesale market operator clears demand and supply

in the network by solving a security constrained economic dispatch (SCED) problem [46] [47], as shown below.

$$max\{\sum_{j\in J} u_j(\hat{P}_j^D) - \sum_{i\in I} C_i(\hat{P}_i^G)\} \tag{16}$$

$$\textbf{s.t: } P_k - P_{gk} + P_{dk} = 0, k = 1, ..., N_{bus} \tag{17}$$

$$|\sum_{k=1}^{N_{bus}} GSF_{bk} \times P_k| \leq F_{max}^b \tag{18}$$

$$\hat{P}_i^G \leq P_i^{max}, i \in I \tag{19}$$

$$\hat{P}_i^G \geq P_i^{min}, i \in I \tag{20}$$

$$u_j(\hat{P}_j^D) = \sum_{l=1}^{L} w_{lj}\hat{P}_{lj}^D \tag{21}$$

$$C_i(\hat{P}_i^G) = a_i\hat{P}_i^G + b_i(\hat{P}_i^G)^2 \tag{22}$$

The notations in SCED algorithm are presented in Table 3. The objective function (16) maximizes the sum of total surplus of all customers and power generation companies. Meanwhile it also minimizes the total generation cost. The first term of equation (16) denotes customers' utility function, while the second term denotes the sum of generation cost. Customer utility function u_j and generator cost function C_i are calculated in equation (21) and (22), respectively. Equation (17) is power supply/demand constraint for each bus. We use λ to denote the multiplier vector of constraints (17). It represents the shadow price of real power balance constraint on each bus. λ corresponds to the LMP in electricity market. Constraint (18) guarantees that the power flow will not exceed the thermal capacity on each transmission line. Constraints (19) and (20) bound the maximum and minimum power output of each generator.

TABLE 3: SCED Algorithm Variables Definition

P_k	bus k power injection	J	aggregated demand bids set
P_{gk}	bus k total generation	I	set of generators
P_{dk}	bus k total demand	$\hat{P}_i^G$	generator i power generation
GSF_{bk}	generation shift factor from bus k to line b		
F_{max}^b	maximum power flow on line b		
N_{bus}	number of buses in the power network		
$\hat{P}_j^D$	dispatched energy consumption of aggregated demand bids set j		
$\hat{P}_{lj}^D$	segment l energy consumption of $\hat{P}_j^D$		
w_{lj}	customer willingness to pay for electricity demand $\hat{P}_{lj}^D$		
P_i^{min}	minimum power output of generator i		
P_i^{max}	maximum power output of generator i		

4.2.2 Substation Dispatching Points Disaggregation

After the wholesale market clears energy demand and supply bidding, the dispatch points need to be disaggregated into individual dispatching instructions for each building to manage its flexible loads. **Algorithm 3** elaborates this procedure, with notations shown in Table 4.

Without considering power losses in distribution system, the disaggregation can be performed for two cases: (1) clearing price is not at the *jump point* of the aggregated demand bid curve, in which case the dispatch quantity for each customer is exactly the energy consumption at clearing price in its demand bid curve; and (2) clearing price falls on the *jump point*, in which case the disaggregated dispatch quantity consists of two parts. The first part is the same as the quantity in case (1) and those quantities will be subtracted from the total dispatch quantity $\boldsymbol{Q}[j]$. Then the remaining dispatch quantity is allocated to each customer proportionally based on their energy demand variation at current clearing price $\boldsymbol{\lambda}[j]$ in its demand bid curve (line 7).

Algorithm 3 $\boldsymbol{q}$ = Dispatch_Disaggregate$(j, \boldsymbol{\lambda}, \boldsymbol{Q})$

1: $\boldsymbol{q} \leftarrow [\boldsymbol{0}]_{1\times n_j}$
2: **for** $k := 1$ to n_j **do**
3: **if** $\boldsymbol{\lambda}[j] \notin \boldsymbol{w_j}$ **then** ▷ *Clearing price is not at jump point*
4: $\boldsymbol{q}[k] \leftarrow \mathcal{P}_{j,k}^d(\boldsymbol{\lambda}[j])$
5: **else** ▷ *Clearing price is at jump point*
6: $\boldsymbol{q}[k] \leftarrow \mathcal{P}_{j,k}^d(\boldsymbol{\lambda}[j])$
7: $+\frac{\overline{P}_{j,k}^{d,\lambda} - \underline{P}_{j,k}^{d,\lambda}}{\sum_{k=1}^{n_j}(\overline{P}_{j,k}^{d,\lambda} - \underline{P}_{j,k}^{d,\lambda})} \cdot \left[\boldsymbol{Q}[j] - \sum_{k=1}^{n_j} \mathcal{P}_{j,k}^d(\boldsymbol{\lambda}[j])\right]$
8: **return** $\boldsymbol{q}$

TABLE 4: Algorithm 3 Variables Definition

$\boldsymbol{q}$	set of disaggregated dispatch quantities
n_j	number of buildings on bus j
$\boldsymbol{Q}$	set of total dispatch quantity on each bus
$\boldsymbol{\lambda}$	set of clearing price on each bus
$\boldsymbol{w_j}$	set of prices in jump points of demand bid curve on bus j
$\mathcal{P}_{j,k}^d$	mapping function between $\boldsymbol{P_{j,k}^d}$ and its bidding prices
$\mathcal{P}_j^D$	mapping function between $\boldsymbol{P_j^D}$ and its bidding prices
$\overline{P}_{j,k}^{d,\lambda}$	maximum energy consumption at price λ in individual demand bid curve k on bus j
$\underline{P}_{j,k}^{d,\lambda}$	minimum energy consumption at price λ in individual demand bid curve k on bus j

4.3 Overall Proactive Demand Participation Algorithm

Based on the methodologies and algorithms introduced in previous subsections 4.1 and 4.2, we summarize the algorithm flow for our proposed proactive demand participation strategy, as show in **Algorithm 4** with notations in Table 5.

TABLE 5: Algorithm 4 Variables Definition

$\boldsymbol{P_r}$	price profile matrix	$\boldsymbol{p_{r_j}}$	price vector on bus j
$\hat{\boldsymbol{D}}$	fixed load demand	N_{bus}	number of buses
$\boldsymbol{\lambda_i}$	set of clearing price on each bus in interval i		
$\boldsymbol{P_j^d}$	energy consumption of individual demand bids set j		
$\boldsymbol{P_j^D}$	energy consumption of aggregated demand bids set j		
$\boldsymbol{Q_i}$	set of total dispatch quantity on each bus in interval i		
$\boldsymbol{q_{i,j}}$	dispatching quantities on bus j in interval i		

As shown in line 5 of Algorithm 4, at current time interval i, Demand_Curve algorithm (Algorithm 1) constructs flexible demand bid curves of individual buildings by solving the MPC formulation in subsection 4.1. Then in line 6, individual demand bid curves are aggregated at substation level (Algorithm 2). The aggregated demand bid curve contains the information of how much electricity

Algorithm 4 $\boldsymbol{P_r} =$ Proactive_Response($\boldsymbol{P_r}$)

1: $\boldsymbol{P_r} = [\boldsymbol{p_{r_1}}, \boldsymbol{p_{r_2}}, ..., \boldsymbol{p_{r_{N_{bus}}}}]^T$
2: **while** $i \leq 24$ **do**
3: **for** each $j \in J$ **do**
4: **for** $k := 1$ to n_j **do**
5: $\boldsymbol{P_j^d} \leftarrow$ Demand_Curve$(i, \boldsymbol{p_{r_j}})$ ▷ *Algorithm 1*
6: $\boldsymbol{P_j^D} \leftarrow$ Bid_Aggregate$(j, \boldsymbol{P_j^d})$ ▷ *Algorithm 2*
7: $(\boldsymbol{\lambda_i}, \boldsymbol{Q_i}) \leftarrow$ SCED$(\boldsymbol{P_j^D}, \hat{\boldsymbol{D}})$
8: **for** each $j \in J$ **do**
9: $\boldsymbol{p_{r_j}}[i] \leftarrow \boldsymbol{\lambda_i}[j]$
10: $\boldsymbol{q_{i,j}} \leftarrow$ Dispatch_Disaggregate$(j, \boldsymbol{\lambda_i}, \boldsymbol{Q_i})$ ▷ *Algorithm 3*
11: **for** $k := 1$ to n_j **do**
12: MPC$(i, \boldsymbol{p_{r_j}}, \boldsymbol{q_{i,j}}[k])$
13: $i \leftarrow i + 1$
14: **return** $\boldsymbol{P_r}$

customers would be willing to buy at different price rates. Based on such information, in line 7, the SCED algorithm introduced in subsection 4.2 determines the economic dispatching points, which contain both electricity market clearing price $\boldsymbol{\lambda_i}$ and dispatch quantity $\boldsymbol{Q_i}$ in interval i. The substation-level dispatching points are disaggregated into dispatch quantity for each individual building customer in line 10 (Algorithm 3). Finally, in line 12 each building operates its flexible load by strictly following the dispatch quantity $\boldsymbol{q_{i,j}}$.

5 Baseline Passive Demand Response

To evaluate our proposed proactive demand response scheme, we compare it with a conventional passive demand response strategy as introduced below. In this baseline passive demand response process, the building energy management system uses the same MPC-based algorithm to schedule HVAC control and battery storage usage, based on the real-time electricity price forecast. Then customers' current energy demand information is submitted to the electricity market operator. Next the electricity market operator is responsible for solving the SCED problem and determining the electricity price for current time interval, given customers' energy demand information.

Fig. 3 illustrates the process of passive demand response strategy for the first three intervals. When scheduling energy demand for the first time interval, the MPC algorithm determines current time interval's optimal flexible load energy demand based on the initial electricity price forecasts. Then the electricity market operator sets the electricity price and updates customers' price forecast profile for current time interval (shown by dash-line shadow). The price forecasts of the rest intervals remain fixed. Next, the predicting window in the MPC algorithm is moved forward by one time interval and the algorithm solves the optimal energy scheduling within the new predicting window. The price forecast profile on the new predicting window is constructed by adding the updated price of last interval at the end of the initial price forecast profile (as shown by solid-line shadow), by assuming the following day's price has a similar characteristic as the corresponding time interval

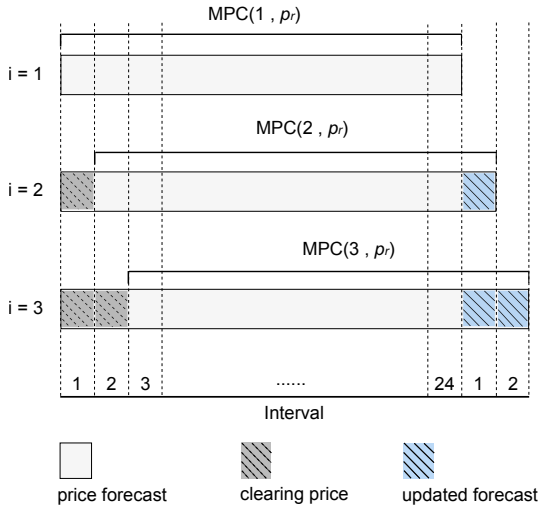

Fig. 3: Passive Demand Response Diagram

at current day. We repeat the above process to obtain the passive demand response in each time interval. The passive demand response algorithm is shown in **Algorithm 5**.

Algorithm 5 $\boldsymbol{P_r} =$ Passive_Response($\boldsymbol{P_r}$)

1: $\boldsymbol{D} = [\boldsymbol{d_1}, \boldsymbol{d_2}, ..., \boldsymbol{d_{N_{bus}}}]^T$
2: $\boldsymbol{P_r} = [\boldsymbol{p_{r_1}}, \boldsymbol{p_{r_2}}, ..., \boldsymbol{p_{r_{N_{bus}}}}]^T$
3: **while** $i \leq 24$ **do**
4: **for** each $j \in J$ **do**
5: $\boldsymbol{d_j} \leftarrow$ MPC$(i, \boldsymbol{p_{r_j}})$
6: $\boldsymbol{\lambda_i} \leftarrow$ SCED$(\boldsymbol{D}, \hat{\boldsymbol{D}})$
7: **for** each $j \in J$ **do**
8: $\boldsymbol{p_{r_j}}[i] \leftarrow \boldsymbol{\lambda_i}[j]$
9: $i \leftarrow i + 1$
10: **return** $\boldsymbol{P_r}$

TABLE 6: Algorithm 5 Variables Definition

$\boldsymbol{P_r}$	price profile matrix	$\boldsymbol{p_{r_j}}$	price vector on bus j
$\boldsymbol{D}$	demand profile matrix	$\boldsymbol{d_j}$	demand vector on bus j
$\hat{\boldsymbol{D}}$	fixed load demand	$\boldsymbol{\lambda_i}$	clearing price in interval i
N_{bus}	number of buses in the power network		

In Algorithm 5, $\boldsymbol{P_r}$ is the electricity price matrix that contains the initial price forecast profile on each bus. $\boldsymbol{D}$ denotes flexible load optimal energy demand matrix, and each of its row stores the optimal energy demand on corresponding bus. In line 5, the MPC algorithm determines the total energy demand d_j within predicting window for each bus based on its own price forecast profile $\boldsymbol{p_{r_j}}$ at time interval i. Line 6 solves the SCED problem to calculate the clearing price for each bus.

6 Experimental Results and Analysis

6.1 Experiment Setup

The IEEE 30-bus network, as shown in Fig. 4, is used to evaluate our proposed proactive demand response scheme. There are six generation plants in this power network. Generator locations and their maximum generation capacities are listed in Table 7.

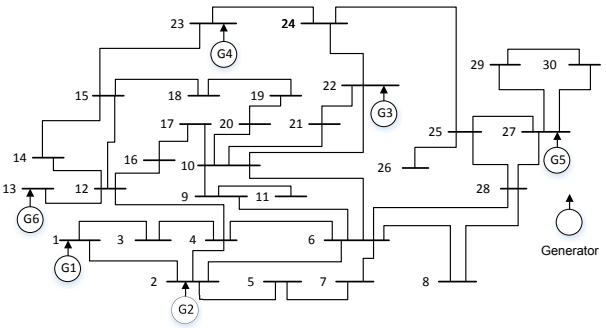

Fig. 4: IEEE 30-Bus Power Network Diagram

TABLE 7: Generator Location and Capacity

Generator	1	2	3	4	5	6
Bus Number	1	2	22	23	27	13
Max(MW)	730	570	1040	700	1600	600

The effectiveness of demand response strategies, including our proactive scheme, directly depends on the amount of flexible energy loads in the power network. To more comprehensively evaluate our scheme, we conduct experiments under different levels of available flexible energy loads (i.e., different amount of HVAC loads and battery storage in our case). Specifically, we define five types of buildings. Each building type has different flexible load ratio (0%, 25%, 50%, 75% and 100%) with respect to the total energy demand – the rest is fixed energy load whose demand profile is given and cannot be changed during scheduling. The flexible load ratio is defined in equation (23), where $D^{flexible}$ is the total energy demand from flexible load and D^{total} is the entire energy demand of a building.

$$R^{flexible} = \frac{D^{flexible}}{D^{total}} \tag{23}$$

In total, 1000 buildings are deployed on each bus. Each building operates an HVAC system and is equipped with a battery storage system. Moreover, each building also has certain amount of fixed load (e.g., lighting and office equipment). Each type of load is characterized by a maximum power demand rating. The total peak demand of all types of load in each building is set to $150kW$. The building's comfort temperature zone range is set to $20\ ^\circ C \sim 23\ ^\circ C$. The battery's maximum charging/discharging rate in one hour is 25% of its maximum capacity, and the battery state-of-charge lower and upper bound is set to 20% and 80% respectively. We calibrate the number of buildings for each building type to obtain various desired flexible load ratios to a bus, as shown below. In (24), m_i denotes the number of the i-th type of building, $R^{flexible}$ is our desired flexible load ratio for the bus.

$$\begin{aligned} &\sum_{i=1}^{5} m_i = 1000 \\ &\frac{\sum_{i=1}^{5} D_i^{flexible} \cdot m_i}{\sum_{i=1}^{5} D_i^{total} \cdot m_i} = R^{flexible} \end{aligned} \tag{24}$$

Furthermore, customers in electricity market are allowed to use different types of demand response strategies, which means some buildings are passive demand response users while some buildings may follow proactive demand response instructions. We define the proactive-demand-response ratio as shown in (25), where $N_{proactive}$ is the number of buildings which participate in proactive demand response scheme and N_{total} is the total number of buildings that contain flexible load in the power network (in our experiments all buildings have the same peak demand. If the buildings are heterogeneous in terms of energy demand as in reality, a more accurate capturing of proactive-demand-response ratio should be based on energy demand rather than number of buildings).

$$R_{proactive} = \frac{N_{proactive}}{N_{total}} \tag{25}$$

In the experiment, a reasonable initial electricity price forecast is constructed by running the passive DR algorithm once. Firstly, each individual building solves the optimal energy demand scheduling for 24 hours based on a real-time price profile. Then the electricity market operator solves the optimal power flow in each interval and derives the initial price forecast that fits with the simulation power network. In practice, time series and artificial intelligence models such as multiple linear regression and artificial neural network models could be used to generate electricity price forecasts.

6.2 Results and Analysis

6.2.1 Effectiveness of Proactive Demand Response

(1) Effect of Proactive-Demand-Response Ratio

We first conduct experiments to study the effect of proactive demand response strategy on system cost at different customer participation levels, assuming the flexible load ratio is 100%. We gradually increase the ratio of proactive-demand-response customers from 0% to 100%, and assume the rest is passive demand response customers. In each case, proactive customers bid for their electricity demand and submit their demand bid curves to wholesale market operator. The system operator performs economic dispatch algorithm to clear the market based on both the flexible demand bids from proactive customers and the rigid demand bids from the passive customers. We calculate the system generation cost in each case, and compare it with the baseline approach where all building customers use passive demand response strategy (i.e., 0% proactive-demand-response ratio).

As shown in Fig. 5, the system generation cost can be *significantly reduced with more proactive demand response participation, and can achieve up to 10% in our experiment*. This clearly demonstrates the advantages of our proactive demand response scheme over passive demand response. When the proactive-demand-response ratio gets very high (exceeding 70% in our example), the reduction curve gets flat as the system has fully leveraged the scheduling potential from proactive customers.

(2) Effect of Flexible-Load Ratio

We then study the effect of flexible load ratio on the power system generation cost, assuming 100% proactive-demand-response ratio. We vary the flexible load ratio from 0% to 100%. For each case, we compare the system generation cost against the baseline passive DR approach. As shown in Fig. 6, our approach again provides significant

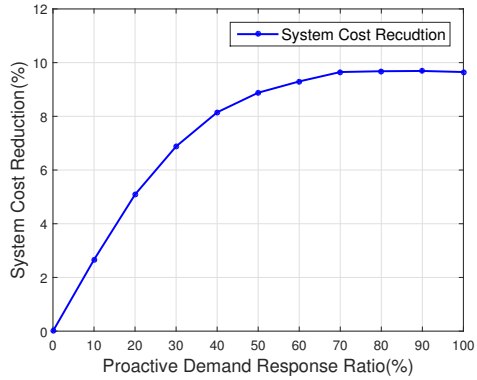

Fig. 5: Power System Generation Cost Reduction under various Proactive Demand Response Ratios

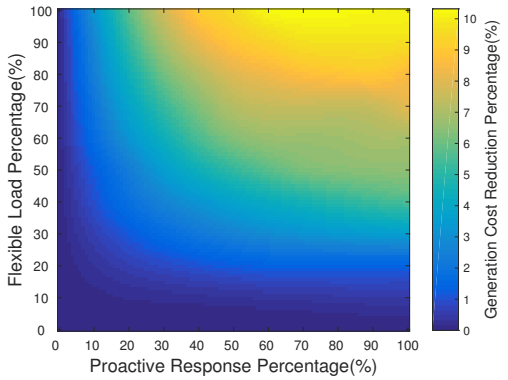

Fig. 7: System Generation Cost Reduction with various Flexible Load Ratios and Proactive Demand Response Ratios

cost reduction with respect to the baseline, and the reduction increases when the flexible load ratio increases.

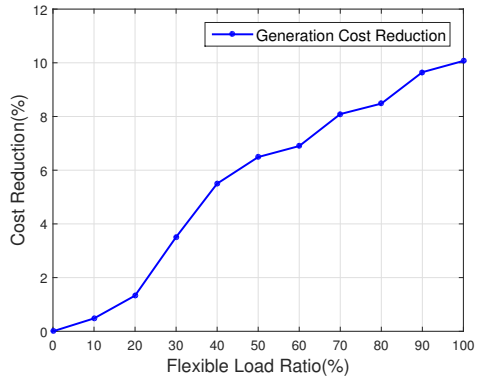

Fig. 6: Power System Generation Cost Reduction under various Flexible Load Ratios

(3) Joint Effect of Proactive-Demand-Response Ratio and Flexible-Load Ratio

We also conduct experiments to evaluate our proactive demand response scheme under various flexible load installment percentage and various proactive customers participation level (essentially a more comprehensive study that includes the previous two aspects). We jointly change the proactive-demand-response ratio and flexible-load ratio, and compare power system generation cost reduction at each setting point versus the baseline case. The results are shown in Fig. 7. The reduction of system generation cost increases when proactive-demand-response ratio increases and/or flexible-load ratio increases.

(4) Electricity Market Pricing

In proactive demand response process, because of the joint optimization of electricity market dispatch and building energy management, the electricity wholesale market operator can fully leverage the advantage of building's flexibility. The market operator can determine the electricity quantity dispatched to each individual customer, instead of just trying to meet customers' energy demand and simply using real-time prices to guide buildings' energy consumption. On the other hand, the decision of buildings' final electricity demand takes power system's generation capacity and operating conditions into consideration by providing market operator more flexibility in demand bid curve and letting market operator decide their electricity consumption. Thus the energy demand on different buses can be appropriately coordinated to avoid the synchronization of customers' peak energy demand. Consequently the proactive demand response scheme can effectively avoid utilizing high-cost generators to supply high power demand.

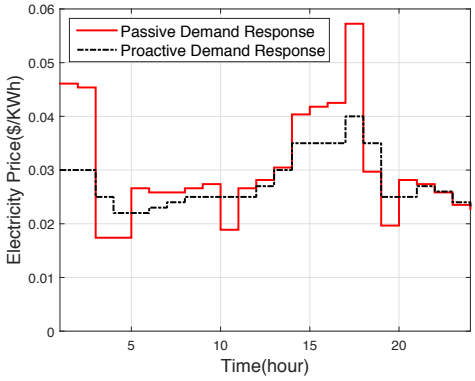

Fig. 8: Clearing Price

In Fig. 8, under 50% of flexible load installment level, the electricity market price profiles in both passive DR process and proactive DR process are presented together. We can see that the price profile in proactive DR is much smoother than that in passive DR. This demonstrates that the *proactive demand response scheme can help mitigate volatility in electricity market pricing*.

6.2.2 Comparison with Iterative RTP Scheme

We have briefly discussed about iterative real-time pricing approaches in Section 2. In this work, we implemented an iterative passive RTP scheme and compared it with our proactive scheme. In the baseline passive demand response strategy introduced in Section 5, we only update the price forecast at each time interval once. In this iterative RTP scheme, there are multiple iterations between the building-side energy scheduling and market clearing in transmission network, following the methodologies from [10]. Specifically, when determining the electricity price for customers

at each time interval, building customers first decide their electricity demands based on the current price forecasts (by solving the MPC-based formulation), and the market operator determines a clearing price in the electricity market after receiving the demands from all buildings. Then the building customers will *repeat* the energy scheduling based on the new price, and the market operator will determine a new price based on the new demands. This process will continue for multiple iterations. In this way, the building-side electricity demand scheduling and the market-side price settling might evolve toward an optimal solution.

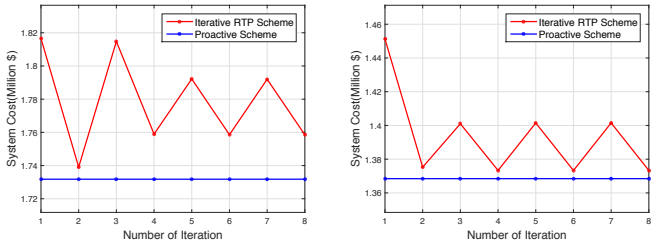

(a) 50% Flexible Load Ratio (b) 100% Flexible Load Ratio

Fig. 9: System Generation Cost Comparison between Proactive Demand Response and Iterative RTP Scheme at Different Flexible Load Ratios: (a) 50% Flexible Load Ratio, (b) 100% Flexible Load Ratio

We conducted experiments to compare the system generation cost of our proactive scheme with the cost of the iterative RTP scheme, under two different levels of flexible load ratios. The results are shown in Fig. 9. From the results we can see that with more iterations, the power system generation cost of iterative RTP scheme may decrease and get close to our proactive scheme, however still higher and oscillating. Such iterative method could be too slow for real-time operations due to high number of iterations.

6.2.3 *Building Customer Incentives from Cost Savings*

In this section, we study the effect of our proactive demand response scheme on building operating cost and evaluate how this might incentivize building customers to participate in the scheme. In passive demand response process, buildings simply schedule their energy demand base on the real-time price forecast at each time interval. Because energy management system in buildings simply manage the electricity consumption in the best interest of their own, a large number of buildings can lead to a very high electricity demand in power grid, which may lead to very high electricity charge rate for customers in return. While in our proactive demand response process, the electricity market operator is trying to maximize all customers' utility and simultaneously minimize the power system generation cost. It will typically make a compromising decision between the two and lead to a relatively low price rate.

Fig. 10 shows the total building operating cost reduction by using proactive DR under different flexible-load ratio levels, compared with the baseline passive DR approach. It demonstrates that building customers may achieve significant operating cost reduction when they leverage their flexible loads and participate in the proactive DR process (in

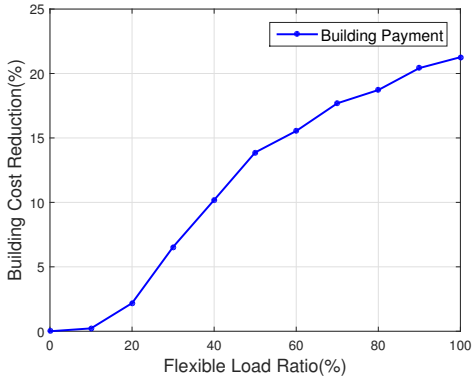

Fig. 10: Building Operating Cost

comparison with the passive approach) . In many commercial and residential buildings, flexible loads such as HVAC systems account for 50% or more of buildings' total energy demand [1], and the flexibility could be even higher when leveraging battery storage. *This shows significant incentives for building customers to participate in the proactive DR scheme.*

6.2.4 *Trade-off between Building Comfort Level and Cost*

Building operating costs and the overall power system generation cost may be significantly impacted by the required building comfort levels. In this section, we study the trade-off between these two aspects. We assume 50% of flexible-load installment level, and gradually relax building's comfort zone boundary by increasing comfort zone temperature range from $2°C$ to $13°C$ (centered around $21.5°C$). This means the building's HVAC system will have more flexibility when regulating the temperature. Then we calculate power system generation cost and total building operating cost for passive and proactive demand response under different comfort zone scenarios.

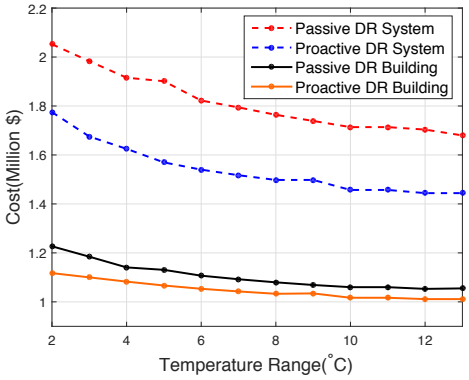

Fig. 11: Trade-off between Building Comfort Zone Temperature Range and Cost (including both Total Building Operating Cost and System Generation Cost)

As shown in Fig. 11, for both passive and proactive demand response strategies, building operating cost and power system generation cost decrease when comfort zone temperature range increases. The results demonstrate that relaxing building's comfort zone requirement can help reduce building customers' operating cost and power system generation cost. The trend should not be surprising, but

the quantitative results could help building operators to trade off between comfort level and energy cost based on occupant activities, operating budget and other factors (e.g., relaxing the comfort zone requirement for conference rooms when no meeting is being held).

6.2.5 Security and Privacy

In our proactive DR scheme, cybersecurity attacks may be conducted by malicious customers to achieve lower operating costs for themselves, similarly as attacks to conventional passive DR strategies [48]. In particular, attackers may manipulate the electricity price forecast signals ($\boldsymbol{P_r}$ in our algorithms) to mislead other customers.

In this work, we conducted preliminary experiments to assess the potential impact of such attack on market clearing price and building operating cost. We assume the customer(s) on bus 16 manipulates the price forecasts on all other buses to mislead their energy usage. Specifically, the attackers significantly increase the price forecast for all other buses (except for 16) at certain periods of the day (6am to 6pm in our experiments), and therefore lead the customers on those buses to schedule their demand to avoid those periods. The attackers on bus 16 will then schedule their own demands on those periods to reduce cost.

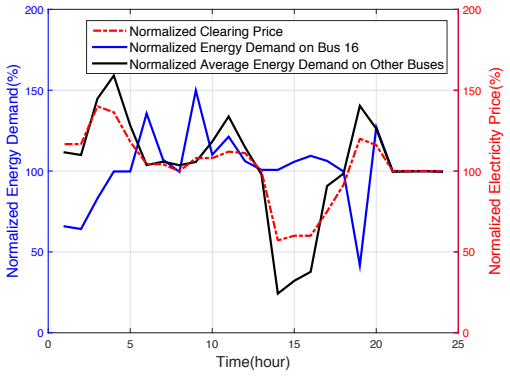

Fig. 12: Normalized Energy Demand and Clearing Price under Price Forecast Manipulation (with respect to Normal Operation without Manipulation)

Fig. 12 shows the *normalized* clearing price and energy demand when price forecast manipulation is conducted by bus 16, compared with normal case without manipulation. The blue and black line represents the normalized energy demand on bus 16 and other buses, respectively. The red curve represents the final market clearing price. We can see that the attackers on bus 16 take advantage of other customers' energy consumption pattern and schedule their heavy load demand to the low price period. Compared with the normal case, attackers on bus 16 are able to reduce their operating cost by 3.85%, while the operating cost for all other customers are increased by 2.1%.

There may also be privacy concerns for our proactive DR scheme. Providing demand bid curves might expose more information of the customers than a simple demand value. However, it is unclear yet what types of user behavior can be learned from such information. We plan to investigate this further in our future work.

6.2.6 Manipulation of Demand Bid Curves

Malicious customers may also submit untruthful demand bid curves to gain benefits for themselves. In this section, we conduct experiments to evaluate the impact of such manipulation of demand bid curves.

We consider the cases where a malicious customer (or multiple colluding customers) has gained control of 50% of the buildings in the network. For simplicity, in this experiment we assume buildings all have the same characteristics (e.g., same flexible load ratio of 50%, same battery storage capacity, etc.), and therefore the malicious customer has control of 50% of the energy demand in the network. In practice it is highly unlikely that such high percentage of demand is under control of malicious customer(s). Nevertheless, we consider it here in our study to investigate how much impact the manipulation of demand bid curves may have in extreme cases.

Fig. 13 shows two manipulated untruthful demand bid curves – in one the bidding price is lowered by 50% and in the other the bidding price is raised by 100% (i.e., 2X). There are many other ways to manipulate the true demand bid curve. We study these two as examples in this work.

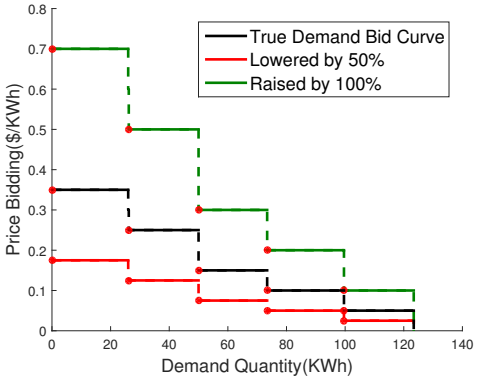

Fig. 13: Manipulated Untruthful Demand Bid Curves

Then, first we consider several cases in which the malicious customer lowers the demand bid curves of *part of the buildings* it controls by 50% at the beginning of peak-load hours (1pm) for an hour. Intuitively, the malicious customer tries to drive the clearing price lower to benefit *the rest of the buildings* it controls. Note that for the part of the buildings that submit untruthful lower demand bid curves at 1pm, they will get lower amount of grid electricity dispatched to them at that hour. Therefore their demand for grid electricity might be higher later on, and their total operating cost might not be lower. However, the malicious customer hopes to achieve an overall reduction of its cost from all of the buildings it controls. Fig. 14 shows the clearing price in different cases, where the malicious customer manipulates 10%, 20%, 30%, 40% and 50% of all the buildings in the market. In the last case the malicious customer basically lowers the demand bid curves of all its controlled buildings at 1pm (note that we assume the malicious customer controls 50% of the buildings in the market).

From Fig. 14, we can see that the more buildings that submit manipulated (lower) demand bids, the lower the clearing price at 1pm is. During the peak hours from 1pm to

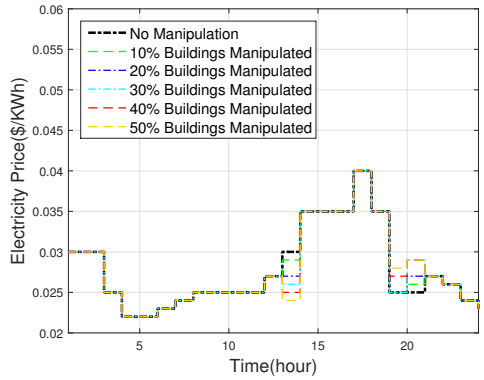

Fig. 14: Clearing Price under Manipulated Demand Bids (Lowered by 50%) in Different Cases

7pm, the clearing price does not change significantly as battery is used to reduce the demand for grid electricity. After 7pm, there is an increase in the clearing price. This confirms our analysis above – the manipulated buildings have to request more energy later to satisfy temperature comfort requirements and battery charging/discharging constraints.

Table 8 shows the total operating cost for the malicious customer and the total cost for the rest of the customers (i.e., the other 50% of the buildings in the network), under the five different cases as explained above. We can see that when the malicious customer manipulates a minority part of its buildings (i.e., 10% and 20% of the total buildings, out of 50% it controls), it gains a very small reduction in its cost; while other customers also see a small reduction. When the malicious customer manipulates more of its buildings, its overall cost starts increasing since the manipulated buildings actually have a higher cost over the whole process.

TABLE 8: Total Costs for Malicious Customer and for Other Customers under Manipulated Demand Bid Curves

	Malicious Customer		Other Customers	
	Cost ($)	Change	Cost ($)	Change
No manipulation	841930	-	841950	-
10% buildings manipulated	841540	↓ 0.05%	841630	↓ 0.04%
20% buildings manipulated	840410	↓ 0.18%	839900	↓ 0.24%
30% buildings manipulated	842140	↑ 0.03%	840950	↓ 0.12%
40% buildings manipulated	844160	↑ 0.27%	841400	↓ 0.07%
50% buildings manipulated	845361	↑ 0.41%	840721	↓ 0.15%

We also conducted similar experiments where the malicious customer raises the demand bid curves by 100% at 1pm for various percentage of the buildings it controls (from 10% to 50% of all buildings in the market). The change of total operating cost is very small – within 0.05% for all cases. We also tried lowering and raising the true demand bid curves for more than one hour during the peak hours (e.g., for the entire peak hours of 1pm to 7pm), and the changes are all relatively minor – within 0.5%. Overall, the manipulations do not lead to a significant cost variation in our experiments. This demonstrates the robustness of our proposed scheme with respect to the manipulation of demand bid curves.

7 Conclusions

This paper proposes an innovative demand response scheme called proactive demand participation. The proactive demand response scheme fully utilizes the flexibility of buildings' energy consumptions and enables individual customers to actively participate in the wholesale electricity market. At the smart building level, an MPC-based HVAC control algorithm is developed for intelligently scheduling HVAC control and battery storage usage. A physical demand bid curve creation algorithm is developed to specify customers' energy consumption preferences under various pricing points. At the wholesale market level, the security constrained economic dispatch problem is formulated to coordinate the operations of power plants and flexible loads. The simulation results demonstrate that the proactive demand response scheme is superior to the conventional passive demand response scheme. The proactive demand response scheme results in higher power system and electricity market efficiency and lower price volatility. From building owners' perspective, the proactive demand participation scheme results in lower building operation cost.

References

[1] "Building energy data book of DOE," *Available: http://buildingsdatabook.eren.doe.gov*.

[2] S. J. Olivieria, G. P. Henzea, C. D. Corbina, and M. J. Brandemuehla, "Evaluation of commercial building demand response potential using optimal short-term curtailment of heating, ventilation, and air-conditioning loads," *Journal of Building Performance Simulation*, vol. 7, no. 2, pp. 100–118, 2014.

[3] N. Yu, Q. Zhu, and T. Wei, "From passive demand response to proactive demand participation," *The 11th annual IEEE International Conference on Automation Science and Engineering*, 2015.

[4] DOE, "Benefits of demand response in electricity markets and recommendations for achieving them," 2006.

[5] FERC, "Assessment of demand response and advanced metering staff report," October 2013.

[6] FERC, "A national assessment of demand response potential," 2009.

[7] M. H. Albadi and E. F. El-Saadany, "Demand response in electricity markets: An overview," *IEEE Power Engineering Society General Meeting*, 2007.

[8] N. Z. John S. Vardakas and C. V. Verikoukis, "A survey on demand response programs in smart grids: Pricing methods and optimization algorithms," *Communications Surveys and Tutorials, IEEE*, vol. 17, no. 1, pp. 152–178, 2015.

[9] A. J. Conejo, J. M. Morales, and L. Baringo, "Real-time demand response model," *IEEE Transactions on Smart Grid*, pp. 236–242, 2010.

[10] N. Li, L. Chen, and S. H. Low, "Optimal demand response based on utility maximization in power networks," *IEEE Power and Energy Society General Meeting*, 2011.

[11] P. Faria and Z. Vale, "Demand response in electrical energy supply: An optimal real time pricing approach," *Energy*, vol. 36, no. 8, pp. 5374–5384, 2011.

[12] P. Yi, X. Dong, A. Iwayemi, C. Zhou, and S. Li, "Real-time opportunistic scheduling for residential demand response," *IEEE Transactions on Smart Grid*, vol. 4, no. 1, pp. 227–234, 2013.

[13] K. Herter, P. McAuliffe, and A. Rosenfeld, "An exploratory analysis of california residential customer response to critical peak pricing of electriicty," *Energy*, vol. 32, no. 1, pp. 25–34, 2007.

[14] G. R. Newsham and B. G. Bowker, "The effect of utility time-varying pricing and load control strategies on residential summer peak electricity use: a review," *Energy Policy*, vol. 38, no. 7, pp. 3289–3296, 2010.

[15] X. C. Yong Liang, Long He and Z.-J. Shen, "Stochastic control for smart grid users with flexible demand," *IEEE Transactions on Smart Grid*, vol. 4, no. 4, pp. 2296–2308, 2013.

[16] R. S. Pedram Samadi, Hamed Mohsenian-Rad and V. W. S. Wong, "Advanced demand side management for the future smart grid using mechanism design," *IEEE Transactions on Smart Grid*, vol. 3, no. 3, pp. 1170–1180, 2012.

[17] M. A. B. Jonathan Wang and W. M. Wang, "Lessons learned from smart grid enabled pricing programs," *Power and Energy Conference at Illinois (PECI), 2011 IEEE*, 2011.

[18] A. Faruqui and J. R. Malko, "The residential demand for electricity by time-of-use: a survey of twelve experiments with peak load pricing," *Energy*, vol. 8, no. 10, pp. 781–795, 1983.

[19] J. Aghaei and M.-I. Alizadeh, "Demand response in smart electricity grids equipped with renewable energy sources: A review," *Renewable and Sustainable Energy Reviews*, vol. 18, pp. 64–72, 2013.

[20] R. H. Ahmad Faruqui and J. Tsoukalis, "The power of dynamic pricing," *The Electricity Journal*, vol. 22, no. 3, pp. 42–56, 2009.

[21] G. Webber, J. Warrington, S. Mariethoz, and M. Morari, "Communication limitations in iterative real time pricing for power systems," *IEEE International Conference on Smart Grid Communications*, 2011.

[22] L. Murphy, R. J. Kaye, and F. F. Wu, "Distributed spot pricing in radial distribution systems," *IEEE Transactions on Power Systems*, vol. 9, no. 1, pp. 311–317, 1994.

[23] J. M. Vignolo and P. M. Sotkiewicz, "Distribution network loss allocation with distributed generation using nodal prices," *Proceedings of the Seventh IASTED International Conference on Power Energy Systems*, 2004.

[24] K. Shaloudegi, N. Madinehi, S. H. Hosseinian, and H. A. Abyaneh, "A novel policy for locational marginal price calculation for distribution systems based on loss reduction allocation using game theory," *IEEE Transactions on Power Systems*, vol. 27, no. 2, pp. 811–820, 2012.

[25] N. G. Singhal and K. W. Hedman, "An integrated transmission and distribution systems model with distribution-based lmp pricing," *North American Power Symposium*, 2013.

[26] L. Xu and R. Baldick, "Transmission-constrained residual demand derivative in electricity markets," *IEEE Transactions on Power Systems*, vol. 22, no. 4, pp. 1563–1573, 2007.

[27] Y. Ma, F. Borrelli, B. Hencey, B. Coffey, S. Bengea, and P. Haves, "Model predictive control for the operation of building cooling systems," *IEEE Transactions on Control Systems Technology*, vol. 20, no. 3, pp. 796–803, 2012.

[28] F. Oldewurtel, A. Parisio, C. N. Jones, M. M. D. Gyalistras, M. Gwerder, V. Stauch, B. Lehmann, and K. Wirth, "Energy efficient building climate control using stochastic model predictive control and weather predictions," *American Control Conference (ACC)*, 2010.

[29] P. Xu, P. Haves, M. A. Piette, and J. Braun, "Peak demand reduction from pre-cooling with zone temperature reset in an office building," *Lawrence Berkeley National Laboratory*, 2004.

[30] M. Maasoumy, A. Pinto, and A. Sangiovanni-Vincentelli, "Model-based hierarchical optimal control design for HVAC systems," *4th ASME Dynamic System Control Conference (DSCC)*, 2011.

[31] M. Maasoumy and A. Sangiovanni-Vincentelli, "Total and peak energy consumption minimization of building HVAC systems using model predictive control," *IEEE Design and Test of Computers*, vol. 29, no. 4, 2012.

[32] M. Maasoumy, Q. Zhu, C. Li, F. Meggers, and A. Sangiovanni-Vincentelli, "Co-design of control algorithm and embedded platform for HVAC systems," *4th IEEE/ACM International Conference on Cyber-Physical Systems (ICCPS)*, 2013.

[33] Y. Yang, Q. Zhu, M. Maasoumy, and A. Sangiovanni-Vincentelli, "Development of building automation and control systems," *IEEE Design and Test of Computers*, vol. 29, no. 4, 2012.

[34] C. J. Baldwin, K. M. Dale, and R. F. Dittrich, "A study of the economic shutdown of generating units in daily dispatch," *IEEE Transactions on Power Apparatus and Systems*, vol. 78, no. 4, pp. 1272–1282, 1959.

[35] J. A. Muckstadt and R. C. Wilson, "An application of mixed-integer programming duality to scheduling thermal generating systems," *IEEE Transactions on Power Apparatus and Systems*, 1968.

[36] N. P. Padhy, "Unit commitment - a bibliographical survey," *IEEE Transactions on Power Systems*, vol. 19, no. 2, pp. 1196–1205, 2004.

[37] T. Shiina and J. R. Birge, "Stochastic unit commitment problem," *International Transactions on Operational Research*, vol. 11, no. 1, pp. 19–32, 2004.

[38] J. Tu, L. Lu, M. Chen, and R. K. Sitaraman, "Dynamic provisioning in next-generation data centers with on-site power production," *the 4-th International Conference on Future Energy Systems (ACM e-Energy)*, 2013.

[39] T. Wei, T. Kim, S. Park, Q. Zhu, S. X.-D. Tan, N. Chang, S. Ula, and M. Maasoumy, "Battery management and application for energy-efficient buildings," *Proceedings of the 51st Annual Design Automation Conference on Design Automation Conference. ACM*, 2014.

[40] T. Wei, Q. Zhu, and M. Maasoumy, "Co-scheduling of HVAC control, EV charging and battery usage for building energy efficiency," *33rd IEEE/ACM International Conference on Computer-Aided Design (ICCAD)*, 2014.

[41] M. Maasoumy, Q. Zhu, C. Li, F. Meggers, and A. Sangiovanni-Vincentelli, "Co-design of control algorithm and embedded platform for HVAC systems," *the 4th IEEE/ACM International Conference on Cyber-Physical Systems (ICCPS)*, 2013.

[42] M. Maasoumy and A. Sangiovanni-Vincentelli, "Modeling and optimal control algorithm design for HVAC systems in energy efficient buildings," *Available: http://www.eecs.berkeley.edu/Pubs/TechRpts/2011/EECS-2011-12.html*, 2011.

[43] C. L. J. Frédéric Bonnans, J. Charles Gilbert and C. A. Sagastizábal, "Numerical optimization: theoretical and practical aspects," in *Springer Science and Business Media*, 2006.

[44] M. Maasoumy, C. Rosenberg, A. Sangiovanni-Vincentelli, and D. Callaway, "Model predictive control approach to online computation of demand-side flexibility of commercial buildings HVAC systems for supply following," *IEEE American Control Conference (ACC 2014)*, June 2014.

[45] N. Yu, H. Sheng, and R. Johnson, "Economic valuation of wind curtailment rights," *IEEE Proceedings, Power and Energy Society General Meeting, Vancouver, British Columbia, Canada*, July 2013.

[46] N. Yu, C.-C. Liu, and J. Price, "Evaluation of market rules using a multi-agent system method," *IEEE Transactions on Power Systems*, vol. 25, no. 1, pp. 470–479, 2010.

[47] N. Yu, C.-C. Liu, and L. Tesfatsion, "Modeling of suppliers learning behaviors in a market environment," *International Journal of Engineering Intelligent Systems*, vol. 15, no. 2, pp. 115–121, 2007.

[48] S. H. Liu Yang and T.-Y. Ho, "Leveraging strategic detection techniques for smart home pricing cyberattacks," *IEEE Transactions on Dependable and Secure Computing*, June 2015.

Tianshu Wei is a Ph.D. Candidate in the Department of Electrical and Computer Engineering at University of California, Riverside, CA, USA. He received a Bachelor degree of Electrical Engineering from Nanjing University, China in 2013. His current research interests are in energy-efficient cyber-physical systems, with a focus on smart buildings and smart grid.

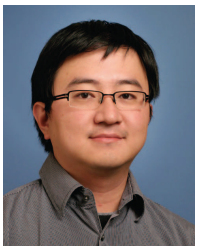

Qi Zhu is an Assistant Professor in the Department of Electrical and Computer Engineering at University of California, Riverside, CA, USA. Prior to joining UCR, He was a research scientist at the Strategic CAD Labs in Intel from 2008 to 2011. He received a Ph.D. in EECS from University of California, Berkeley in 2008, and a B.E. in CS from Tsinghua University in 2003. His research interests include model-based design and software synthesis for cyber-physical systems, CPS security, energy-efficient buildings and infrastructures, and system-on-chip design.

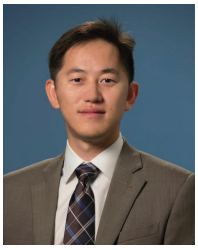

Nanpeng Yu (M'11) received the M.S. and Ph.D. degree in electrical engineering from Iowa State University, Ames, IA, USA in 2007 and 2010 respectively. He was a Senior Power System Planner and Project Manager at Southern California Edison, Rosemead, CA, USA, from 2011 to 2014. He is currently an Assistant Professor of Electrical and Computer Engineering at University of California, Riverside, CA, USA. His current research interests include electricity market design and optimization, big data analytics in power systems, demand response, and energy storage valuation.